

The structure of human olfactory space

Alexei A. Koulakov^{1*}, Armen G. Enikolopov^{1,2}, and Dmitry Rinberg³

¹*Cold Spring Harbor Laboratory, Cold Spring Harbor, NY 11724*

²*Department of Biological Sciences, Columbia University, New York, NY 10027*

³*HHMI Janelia Farm Research Campus, HHMI, Ashburn, VA 20147*

*Correspondence: koulakov@cshl.edu

We analyze the psychophysical responses of human observers to an ensemble of monomolecular odorants. Each odorant is characterized by a set of 146 perceptual descriptors obtained from a database of odor character profiles. Each odorant is therefore represented by a point in highly multidimensional sensory space. In this work we study the arrangement of odorants in this perceptual space. We argue that odorants densely sample a two-dimensional curved surface embedded in the multidimensional sensory space. This surface can account for more than half of the variance of the psychophysical data. We also show that only 12% of experimental variance cannot be explained by curved surfaces of substantially small dimensionality (<10). We suggest that these curved manifolds represent the relevant spaces sampled by the human olfactory system, thereby providing surrogates for olfactory sensory space. For the case of 2D approximation, we relate the two parameters on the curved surface to the physico-chemical parameters of odorant molecules. We show that one of the dimensions is related to eigenvalues of molecules' connectivity matrix, while the other is correlated with measures of molecules' polarity. We discuss the behavioral significance of these findings.

INTRODUCTION

Our current understanding of many sensory modalities is based on knowledge of the underlying sensory spaces. For example, visual stimuli are well described by their position and the spectral content of the light emitted/scattered by them. The somatosensory system represents positions of stimuli relative to the body surface, which leads to the body-centric somatosensory world. Our understanding of the sense of smell is hindered by the lack of a well-defined perceptual space and knowledge of how this space is related to the properties of odorant molecules¹⁻².

It is quite easy to build a generalist olfactory space. Every monomolecular component of a complex odor can be viewed as an individual dimension with the coordinate along this dimension determined by a concentration of the given component. The number of dimensions in this space is equal to the number of monomolecular chemical compounds that can be

presented to the olfactory system. Every odorant can be placed uniquely in such a generalist olfactory space. Although the space is complete, it is too large to be relevant to human observers. This is simply because the brain does not have enough olfactory receptors to sample the generalist space in its entirety. The olfactory system is likely to sample a more specialist, lower dimensionality subspace of the general space. The structure of the relevant sensory subspace can be derived from various properties of the olfactory system and is the topic of this and prior studies³⁻⁵.

Here we investigate the structure of olfactory space defined by the responses of human observers. We base our analyses on the Atlas of Odor Character Profiles (AOCP)⁶, a database of psychophysical responses of human observers to an array of odorants. In the course of our analyses we discovered that odorants in human olfactory space accumulate near a 2D curved manifold (a curved surface that can be locally approximated by a plane).

The 2D manifold accounted for 51% of the variability in the experimental data. This finding prompted us to seek an approximation to the sensory space in the form of curved continuous surfaces of higher dimension. We show that an approximation of these responses with continuous spaces of sufficiently low dimensionality higher than two could account for 81% of the variability in experimental data. We also find that the intrinsic statistical variability in the data is at least 7%. Thus, only the remaining variance of 12% or less can be attributed to discontinuous features in the sensory space. We argue therefore that a curved continuous manifold of sufficiently low dimension carries most of the information about known features of human olfactory perception.

RESULTS

The AOCIP database contains information about responses of human observers to 144 monomolecular odorants. Each odorant is characterized by a set of 146 psychophysical descriptors, such as ‘fruity’, ‘floral’, ‘sickening’, ‘warm’, etc. (see Supplementary Material for complete list of odorants and descriptors). Thus, each odorant/descriptor pair is characterized by the percentage of observers that recognized the descriptor as applying to odorant. The database can therefore be viewed as a set of 144 points representing individual odorants positioned in a 146-dimensional space of psychophysical descriptors. The resultant cloud of 144 points placed into the multidimensional space of descriptors contains vast information about human perception of monomolecular odorants.

To visualize the multidimensional cluster of odorants we used principal component analysis (PCA). This technique determines directions in the 146D descriptor space that account for the greatest proportion of data variance. These directions [principal components (PCs)] are recognized as the least redundant dimensions and thereby the most informative about the data set⁷. The cluster of 144 odorants projected onto a 3D space specified by the first three principal components is shown in Figure 1A and B. To characterize the amount of information missing from the PCA projection it is customary to present the fraction of variance that is included in the low-dimensional representation (Figure 1E). The 3D PCA projection in Figure 1A includes 52% of the

variance in the original data. 48% of the data variance is therefore excluded from 3D representation. The value of PCA in our analysis is in visualizing the correlations present in the data rather than in accounting for these correlations.

Odorants projected to 3D PC space when viewed from certain direction clustered near a C-shaped curve, suggesting that the data points reside close to a 2D surface (Figure 1B). We therefore fitted the set of points by the smooth curved surface shown in Figure 1C and D. The best fit was obtained in 146D space by minimizing the distances from the data points to the nearest points on the surface. To capture the curvature of the surface, it was defined by a second-order polynomial function of 2 parameters: the first PC and a linear combination of the second and the third PCs. The 2D curved surface (manifold) accounted for 94% of the data variance projected to the three principal components (Figure 1A and B) and 56% of the data variance contained in the entire data set containing 146 dimensions.

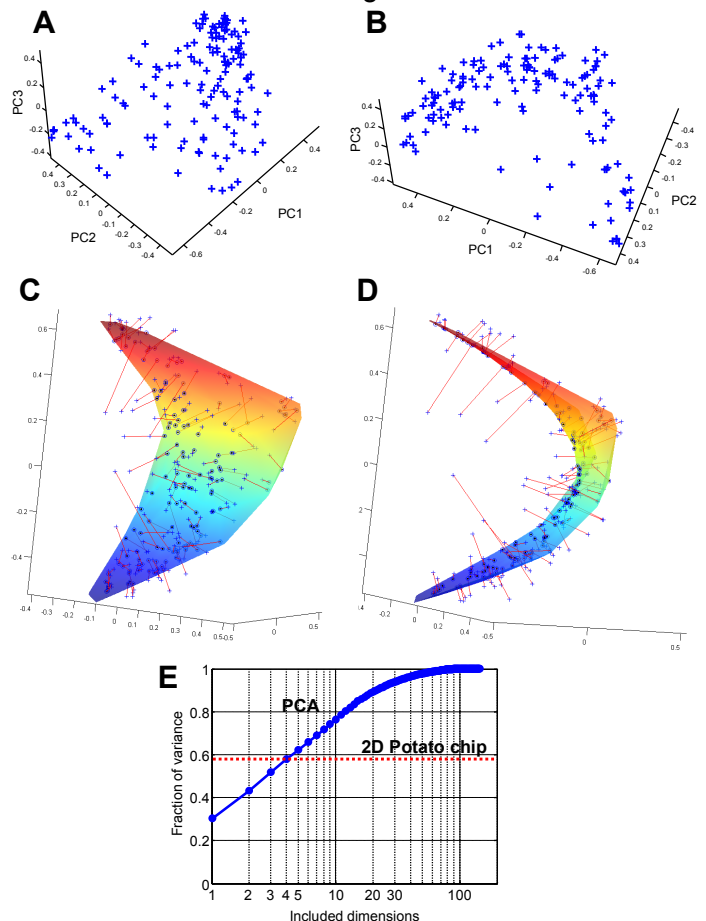


Figure 1. Odorants in the PCA space. (A) Each of 144 odorants can be represented as a point in the 146D space of psychophysical descriptors. The odorants are shown by blue crosses placed in the 3D space of principal components. (B) When viewed from certain direction, the odorants clustered near a C-shaped 1D curve, suggesting that in 3D the odorants are distributed close to a 2D curved surface. (C and D) The 2D surface representing the best fit to the data. The odorants (blue crosses) are connected to the nearest points on the surface by the red lines representing the residual errors. The 2D surface minimizes the total squared length of the residuals computed in 146D. The total squared length of residuals can be viewed as remaining variance in the data not accounted for by the projection to the 2D curved manifold. (E) The fraction of included variance as a function of the number of PCA dimensions. The fraction of variance accounted by the 2D curved manifold in (C) and (D) is 56% (red dotted line).

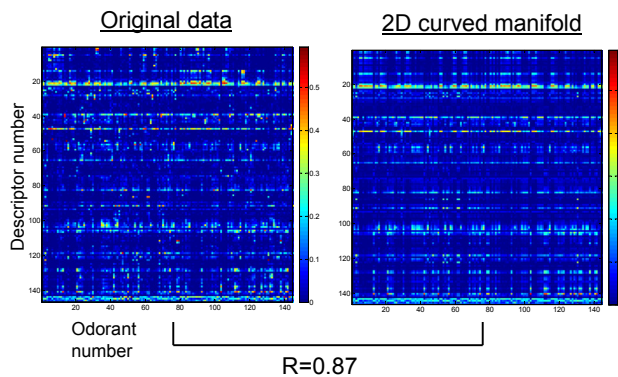


Figure 2. Comparison between original psychophysical data and its projection on to 2D curved manifold. Images represent the coordinates (color coded) of 144 odorants in 146D space of descriptors for (A) original data, blue crosses in Figure 1 C&D and (B) its projections to 2D curved manifold, circles in Figure 1 C&D.

How well does a 2D curved manifold in 146D space predict the responses of human observers? To answer this question we compared the original data and its projection to a 2D curved surface (Figure 2). The projections were defined as the nearest points on the 2D surface to a given odorant, as illustrated in Figure 1C and D. The comparison of the two sets of points yielded a correlation coefficient of 87%. Because some correlation is introduced by the average responses to a given descriptor (horizontal bands in Figure 2), we also obtained the correlation coefficient when the averages are excluded from the matrices. This procedure resulted in a correlation coefficient of 75% between the original data and the 2D projection. We conclude that the 2D curved space yields a potent approximation to the psychophysical

responses of human observers and therefore forms a reliable surrogate for human olfactory sensory space. We next determined what descriptors contribute to the two parameters on the surface. The first parameter (elevation) is associated with the first PC of the data. As has previously been suggested, this parameter could be correlated with the pleasantness or perceptual valence of odorants^{3-4,8}. Consistent with this observation, we find that the psychophysical descriptors that contribute to the first coordinate with large positive/negative coefficients are associated with repulsive/attractive odorant properties (see top and bottom of Figure 3 for the 10 descriptors with the largest positive/negative coefficients, respectively). The second coordinate on the 2D manifold (azimuth) was obtained as a linear combination of the second and the third PCs. The psychophysical descriptors contributing with large coefficients to this coordinate are listed in Figure 3 too (left and right). A possible significance of the second coordinate is discussed below.

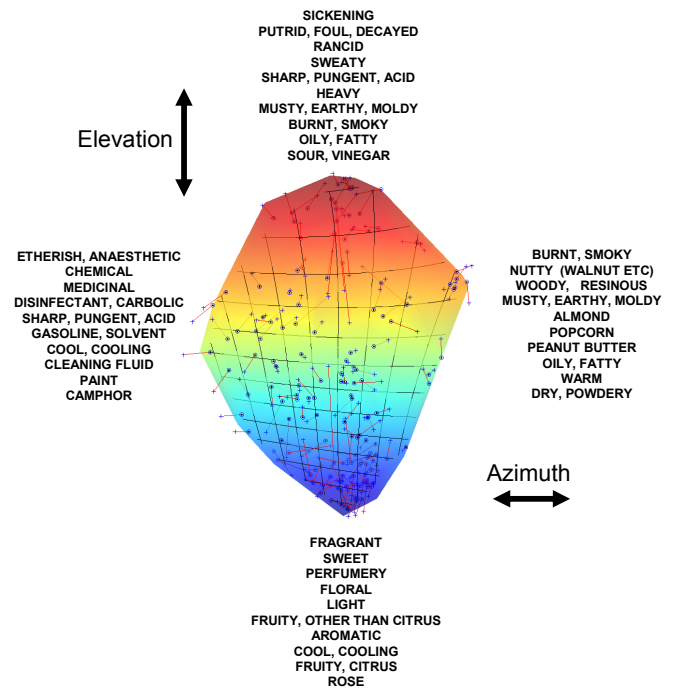


Figure 3. Psychophysical descriptors that contribute with large positive/negative coefficients to the coordinates on the 2D surface. The two coordinates are defined as elevation and azimuth as indicated.

Could a curved manifold of dimensionality higher than two characterize human olfactory space more fully? Because we use second order polynomials in our approximation, the number of parameters of the

regression is proportional to square of the number of dimensions. To avoid overfitting, we used the jackknife procedure⁹ (see Methods for details). In this procedure, a single odorant is removed from the database, an approximation is calculated based on remaining entries in the database, and the result is compared with the odorant that is left out. Our results show that a space of sufficiently small dimensionality (≤ 10) can account for a substantial fraction of variance in the experimental data (up to 81%, Figure 4A). The resulting continuous spaces also allow a substantial correlation with experimental data. Thus, when the experimental data are ‘projected’ to smooth curved manifolds of varying dimensionality by finding the nearest points on the manifold, the correlation between the data and projections can reach 90% or 94% (Figure 4B). These two results are obtained for data sets in which the means of the rows are subtracted/included respectively (Figure 2) and, therefore the data are centered/non-centered with respect to each of the 146 perceptual dimensions.

We found therefore that about 81% of the variance in the dataset is captured by the smooth curved manifolds. We also estimated the errors present in the data due to a finite number of human subjects contributing to the dataset to be about 7%. We conclude that only about 12% of the variance in the experimental data cannot be captured by continuous curved manifolds of dimensionality ≤ 10 . Most (51%) of the experimental variance is reproduced by the 2D curved surface considered above.

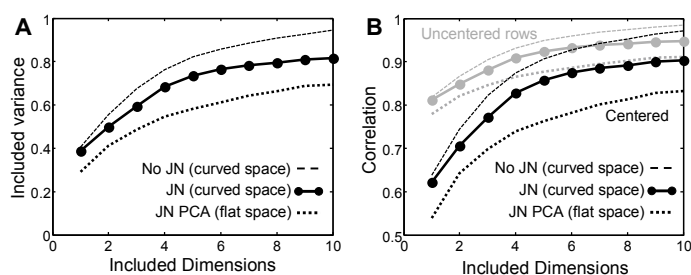


Figure 4. Approximation of psychophysical responses with spaces of small dimensionality. To avoid overfitting we applied jackknife (JN) technique. The results for best function/flat spaces are shown by solid/dotted lines as a function of number of dimensions included. The flat space technique is equivalent to PCA and is shown for comparison. (A) The variance of dataset accounted by the low-dimensional representation. 2D curved manifold

accounted for 51% of experimental variance. (B) Pearson correlation as a function of surface dimensionality.

We then attempted to establish the relationship between the two perceptual dimensions (elevation and azimuth) and the physico-chemical properties of odorants. To this end it is necessary to refine the definition of perceptual coordinates on the surface. As seen in Figure 3, the odorants tend to accumulate near the poles of the 2D surface (large positive and negative values of elevation). To remove this singularity we found a non-linear (quadratic) transformation that makes the density of odorants approximately uniform throughout the surface. The new coordinate grid is displayed in Figure 3 on the 2D manifold. The resulting two coordinates on the surface, elevation and azimuth, were then compared to various physico-chemical and structural properties of odorants. 72 physico-chemical properties were obtained from the computer package Molecular Modeling Pro¹⁰. The structural descriptors included 7 atom counts, 16 pair counts, and 31 triples counts obtained from structural formulas of odorants. The total physico-chemical/structural space included 126 properties for each molecule. We then applied a greedy algorithm developed by Refs. [9,11] to find which properties correlate best with the two perceptual dimensions. The greedy algorithm is an iterative procedure that increases the number of included properties one by one. On each step a new property is added if it results in a maximum increase of Pearson correlation coefficient with a given perceptual dimension. The results of this analysis, physico-chemical properties that yield the best correlation with both azimuth and elevation are presented in Table 1 as a function of the number of included physico-chemical properties (iteration steps).

Table 1. Physico-chemical and structural properties of odorant molecules that contribute most strongly to the two perceptual dimensions. CIM is Chemical intuitive molecular index. Order is the number of dimensions included. R is Pearson correlation coefficient.

| Elevation | | | Azimuth | |
|-----------|-----------------|------|----------------------|------|
| Order | Name | R | Name | R |
| 1 | Burden CIM8 | 0.53 | Water of hydration | 0.33 |
| 2 | C-S pairs | 0.59 | Normal melting point | 0.38 |
| 3 | N count | 0.63 | Debye dipole moment | 0.42 |
| 4 | Molecular width | 0.66 | H-S pairs | 0.44 |
| 5 | H-C-O triples | 0.68 | Dispersion 3D | 0.47 |

The elevation coordinate on the surface is correlated with structural properties of the molecules, such as Burden chemical intuitive molecular indices (CIMs), which represent eigenvalues of the connectivity matrix¹⁰. These eigenvalues represent simple surrogates for the solution of the quantum-mechanical Hamiltonian equation. We found that all CIMs (1 through 10) are generally well correlated with the elevation coordinate. We also found that simple carbon atom number yields almost the same correlation as CIMs ($R=0.50$, see Supplementary Material for more detail). For the azimuth coordinate we find that the correlated variables are descriptive of molecules' polarity or hydrophobicity. Thus, four of the five best correlated properties in Table 1 for azimuth depend on molecules' polarity, including melting point temperature. We conclude that the azimuth on the 2D curved manifold is correlated with the hydrophobicity or polarity of odorant molecules.

DISCUSSION

In this study we showed that a smooth curved surface of substantially small dimensionality can successfully approximate the responses of human observers to a variety of monomolecular odorants. A 2D curved surface can account for most of the variance in behavioral data. In agreement with previous studies^{3-4,8,12}, we suggest that one of the dimensions on the 2D surface is the pleasantness or perceptual valence of the odorants. This dimension is correlated with some physico-chemical properties of the molecules, such as the count of the carbon atom count or eigenvalues of the connectivity matrix associated with the structural formula (CIMs¹⁰). The second perceptual dimension is correlated with the measures of polarity or hydrophobicity, such as water of hydration, normal melting point temperature, etc (Table 1). Because mammalian Class I olfactory receptors (ORs) are related to fish ORs that are expected to bind water-soluble compounds¹³, the second dimension may be detected by the difference in responses of the two classes of olfactory receptors: Class I and II. The importance of differentiation between two classes of receptors is highlighted in the mammalian olfactory system by their anatomical segregation¹⁴⁻¹⁵. The perceptual significance of this second coordinate (dimension) is less straightforward.

An intriguing possibility for the second perceptual coordinate is suggested by studies of cross-modal correlations of smells and sounds. It is reported for example that some Amazonian tribes recognize synesthetic coupling of music and smells¹⁶. An association between auditory pitch and odorant quality has been proposed for a long time¹⁷⁻¹⁹. The arrangement of smells as a function of auditory frequency or pitch was shown to be consistent between human subjects¹². Most importantly, this arrangement was shown to be independent of the pleasantness of odorants¹². The latter observation suggests an interpretation of the second olfactory dimension (azimuth) as related to the auditory pitch of sounds synesthetically associated with the odorants. This is because this dimension is perpendicular (decorrelated) to pleasantness (elevation) and is the second most significant dimension of olfaction. In agreement with this interpretation, the second dimension emerges from differentiation between groups of psychophysical descriptors that include 'burnt', 'oily', 'fatty' and the group including 'etherish', 'chemical', and 'medicinal'.

The two dimensions of olfaction studied here could mediate two different escape behaviors important for humans. Thus, the pleasantness dimension (elevation) could mediate the escape from products of bacterial decay. Descriptors that are important to this dimension include 'putrid', 'foul', 'decayed', 'rancid', etc. On the other hand, the second dimension (azimuth) could be important for detection of carcinogens in burnt food. These substances known as heterocyclic amines are formed during the cooking of meat, by condensation of creatinine with amino acids²⁰. The set of descriptors significant for the second dimension ('burnt', 'smoky') is in agreement with this interpretation.

The low dimensionality of the olfactory space reported here does not eliminate the complexity of olfactory percepts. Indeed, if one adopts a 2D approximation to olfactory space, odor identity depends only on two parameters. But the surface buckles into all 146 dimensions due to its curvature. Thus, although a correlation is present in the data that allows us to reduce the dimensionality of the dataset, olfactory percepts remain complex and varying in all 146 dimensions.

We report here that the human perceptual space of monomolecular odorants can be viewed as continuous, curved, and low-dimensional. Most of the variance in the perceptual data is captured by a 2D curved surface. The two dimensions of the surface can be related to physic-chemical properties of odorant molecules such as an eigenvalue of the odorant molecule connectivity matrix and the polarity of the molecules respectively.

METHODS

Responses to odorants. Responses to 144 odorants were obtained from Ref. [6] and represented in a set of 146D vectors \vec{r}_i ($i=1\dots 144$). We used PU set of responses from Ref [6]. PU (percent used) describes the fraction of about 150 observers that thought that a given descriptor applies to an odorant. We verified that our conclusions do not change substantially if other parameters are used instead of PU. We performed PCA on the vectors using SVD procedure. All computations were performed using MATLAB (Mathworks, Inc.). Before applying PCA we normalized response vectors to have unit length in terms of L_2 measure. This implies that the vectors resided on a unit sphere in 146D. This reduced somewhat the dimensionality of the dataset to 145D. The normalization step was intended to equalize the odorants in their perceived intensity or concentration. We verified that our conclusions do not change qualitatively if other measures (L_2 through L_9) are used for normalization. We noticed some deterioration of the fits beyond this range.

Approximating odorant response with curved spaces. Each odorant vector \vec{r}_i was approximated with the ‘projected’ vector \vec{p}_i . Here index i enumerates the odorants while each vector contains 146 components corresponding to psychophysical descriptors. The projected vectors were sought in the form

$$\vec{p}_i = \vec{A} + \sum_{\alpha=1}^D \vec{B}_{\alpha} x_{\alpha i} + \sum_{\alpha=1}^D \sum_{\beta=1}^D \vec{C}_{\alpha\beta} x_{\alpha i} x_{\beta i}. \quad (1)$$

Here \vec{A} , \vec{B}_{α} , and $\vec{C}_{\alpha\beta}$ are odorant-independent parameters of the surface. Parameters $\vec{C}_{\alpha\beta}$ allowed the surface to be curved. Parameters $x_{\alpha i}$ define positions of odorants on the surface. D is the

number of parameters per odorant which is the dimensionality of the surface. The manifold defined by this equation is D -dimensional. In figure 2 we used $D=2$, while in Figure 4 the dimensionality was varied. To find \vec{A} , \vec{B}_{α} , $\vec{C}_{\alpha\beta}$, and $x_{\alpha i}$ we minimized

$$\sum_i \|\vec{r}_i - \vec{p}_i\|^2$$

using conjugate gradient algorithm. The set of parameters $x_{\alpha i}$ was determined therefore as the nearest points on the curved manifold. The nearest points define ‘projections’ onto the curved manifold.

Jackknife procedure. Approximating human psychophysical responses with higher dimensional curved manifolds is confounded by a dramatic increase in the number of parameters of fit. Because the number of parameters increases as a second power of the number of dimensions in our quadratic regression, for a moderately low-dimensional manifold we find that we can perfectly fit all of the experimental data (Figure 4A, dashed line). To avoid this overfitting problem we employed the jackknife technique, in which we remove a single odorant from the perceptual database, obtain a high-dimensional fit for the responses to the remaining compounds, and calculate the distance between the fitted manifold and the removed odorant. By applying this procedure for all odorants in the database sequentially we evaluated a variance of the approximation with curved manifolds. The variance does not vanish for spaces of high dimensionality due to overfitting (Figure 4A, solid line).

The natural system of coordinates of the 2D surface was used to equilibrate the density of odorants (grid in Figure 3). The odorants were projected to 2D PCA space and the Delaunay triangulation was calculated. The edges of triangulation were replaced with elastic strings of unit equilibrium length and a coordinate transformation was found that minimizes the elastic energy of the strings. The coordinate transformation was constrained to the form used above [equation (1)] with the mapping of 2D to 2D space. The results are shown in the Supplementary Material.

Estimating the variability due to a finite number of observers. The psychophysical variable used here (percent used, PU) is convenient for estimating the experimental variability. We resampled the data for every entry in the database independently using 149 observers as specified in Ref. [6]. We estimated

the variance of the resulting ensemble to be equal to 7% of the experimental variance present in Ref. [6].

Physico-chemical parameters. The values of 72 parameters were calculated using the program Molecular Modeling Pro™ (ChemSW, Fairfield, CA). We verified that the use of 1999 parameters generated by E-Dragon (VCCLAB.org) did not improve the result suggesting a redundancy in the data. We used logarithms of all the parameter values normalized to a unit variance and zero mean for each parameter across odorants.

REFERENCES

1. Cain, W.S. History of research on smell. in *Handbook of perception*, Vol. VIA (eds. Carterette, E.C. & Friedman, M.P.) 197-229 (Academic Press, New York, 1978).
2. Wise, P.M., Olsson, M.J. & Cain, W.S. Quantification of odor quality. *Chem Senses* **25**, 429-443 (2000).
3. Berglund, B., Berglund, U., Engen, T. & Ekman, G. Multidimensional analysis of twenty-one odors. *Scand J Psychol* **14**, 131-137 (1973).
4. Jones, F.N., Roberts, K. & Holman, E.W. Similarity judgments and recognition memory for some common spices. *Percept Psychophys* **24**, 2-6 (1978).
5. Lapid, H., Harel, D. & Sobel, N. Prediction models for the pleasantness of binary mixtures in olfaction. *Chem Senses* **33**, 599-609 (2008).
6. Dravnieks, A. & ASTM Committee E-18 on Sensory Evaluation of Materials and Products. Section E-18.04.12 on Odor Profiling. *Atlas of odor character profiles*, (ASTM, Philadelphia, PA, 1985).
7. Jolliffe, I.T. *Principal component analysis*, (Springer, New York, 2002).
8. Khan, R.M., *et al.* Predicting odor pleasantness from odorant structure: pleasantness as a reflection of the physical world. *J Neurosci* **27**, 10015-10023 (2007).
9. Saito, H., Chi, Q., Zhuang, H., Matsunami, H. & Mainland, J.D. Odor coding by a Mammalian receptor repertoire. *Sci Signal* **2**, ra9 (2009).
10. Burden, F.R. A chemically intuitive molecular index based on the eigenvalues of a modified adjacency matrix. *Quant Struct-Act Rel* **16**, 309-314 (1997).
11. Haddad, R., Carmel, L., Sobel, N. & Harel, D. Predicting the receptive range of olfactory receptors. *PLoS Comput Biol* **4**, e18 (2008).
12. Belkin, K., Martin, R., Kemp, S.E. & Gilbert, A.N. Auditory pitch as a perceptual analogue to odor quality. *Psychological Science* **8**, 340-342 (1997).
13. Zhang, X. & Firestein, S. The olfactory receptor gene superfamily of the mouse. *Nat Neurosci* **5**, 124-133 (2002).
14. Bozza, T., *et al.* Mapping of class I and class II odorant receptors to glomerular domains by two distinct types of olfactory sensory neurons in the mouse. *Neuron* **61**, 220-233 (2009).
15. Tsuboi, A., Miyazaki, T., Imai, T. & Sakano, H. Olfactory sensory neurons expressing class I odorant receptors converge their axons on an antero-dorsal domain of the olfactory bulb in the mouse. *Eur J Neurosci* **23**, 1436-1444 (2006).
16. Classen, C. Sweet colors, fragrant songs: Sensory models of the Andes and Amazon. *American Ethnologist* **17**, 722-735 (1990).
17. Piesse, C.H. *Piesse's art of perfumery*, (Piesse and Lubin, London, 1881).
18. Juhász, A. Über eine neue Eigenschaft der Geruchsempfindungen. *Bericht über den IX Kongress für Experimentelle Psychologie in München* **9**(1926).
19. von Hornbostel, E.M. Über Geruchshelligkeit. *Pflügers Archiv European Journal of Physiology* **227**, 517-538 (1931).
20. Report on Carcinogens, Eleventh Edition; U.S. Department of Health and Human Services, Public Health Service, National Toxicology Program .

SUPPLEMENTARY MATERIAL

The Structure of Human Olfactory Space

by Alexei A. Koulakov, Armen G. Enikolopov, and Dmitry Rinberg

1. Odorants included in the analysis

The following odorants were used from the Atlas of Odor Character profiles.

| | | |
|----|------------|---|
| 1 | 698-10-2 | Abhexone |
| 2 | 98-86-2 | Acetophenone |
| 3 | 1122-62-9 | Acetyl Pyridine: ortho-Acetyl Pyridine |
| 4 | 141-13-9 | Adoxal |
| 5 | 77-83-8 | Aldehyde C-16 (So-Called)→ Lower Concentration |
| 6 | 77-83-8 | Aldehyde C-16 (So-Called)→ Higher Concentration |
| 7 | 104-61-0 | Aldehyde C-18 (So-Called) |
| 8 | 123-68-2 | Allyl Caproate |
| 9 | 123-82-2 | Amyl Acetate: iso-Amyl Acetate |
| 10 | 540-18-1 | Amyl Butyrate |
| 11 | 60763-41-9 | → Amyl Cinnamic Aldehyde Diethyl Acetal |
| 12 | 102-19-2 | → Amyl Phenyl Acetate |
| 13 | 2173-56-0 | → Amyl Valerate |
| 14 | 29597-36-2 | → Andrane |
| 15 | 104-46-1 | → Anethole |
| 16 | 100-66-3 | → Anisole |
| 17 | 89-43-0 | → Auralva |
| 18 | 100-52-7 | → Benzaldehyde |
| 19 | 119-84-8 | → Benzo Dihydro Pyrone |
| 20 | 5655-61-8 | → Bornyl Acetate: iso-Bornyl Acetate |
| 21 | 107-92-6 | → Butanoic Acid |
| 22 | 71-38-3 | → Butanol: 1-Butanol |
| 23 | 544-40-1 | → Butyl Sulfide |
| 24 | 67634-06-4 | → Butyl Quinoline: iso-Butyl Quinoline |
| 25 | 78-22-2 | → Camphor: dl-Camphor |
| 26 | 99-49-0 | → Carvone: l-Carvone |
| 27 | 87-44-5 | → Caryophyllene (beta and gamma Isomers) |
| 28 | 33704-61-9 | → Cashmeran |
| 29 | 17369-59-4 | → Celeriax |
| 30 | 89-68-9 | → Chlorothymol |
| 31 | 104-55-2 | → Cinnamic Aldehyde |
| 32 | 141-27-5 | → Citral |
| 33 | 5585-39-7 | → Citralva |
| 34 | 91-64-5 | → Coumarin |
| 35 | 108-39-4 | → Cresol: m-Cresol |
| 36 | 106-44-5 | → Cresol: p-Cresol |

- 37 140-39-6 → Cresyl Acetate: p-Cresyl Acetate
- 38 103-93-5 → Cresyl Butyrate: p-Cresyl-iso-Butyrate
- 39 104-93-8 → Cresyl Methyl Ether: p-Cresyl Methyl Ether
- 40 122-03-2 → Cuminic Aldehyde
- 41 1423-46-7 → Cyclocitral: iso-Cyclocitral
- 42 55704-78-4 → Cyclodithalfarol
- 43 765-87-7 → Cyclohexanedione: 1,2-Cyclohexanedione
- 44 108-93-0 → Cyclohexanol
- 45 80-71-7 → Cyclotene
- 46 67634-23-5 → Cyclotropal
- 47 25152-84-5 → Decadienal: 2,4-trans-trans-Decadienal
- 48 91-17-8 → Decahydro Naphthalene
- 49 111-92-2 → Dibutyl Amine
- 50 352-93-2 → Diethyl Sulfide
- 51 10094-34-5 → Dimethyl Benzyl Carbonyl Butyrate
- 52 103-05-9 → Dimethyl Phenyl Ethyl Carbinol
- 53 5910-89-4 → Dimethyl Pyrazine: 2,3-Dimethyl Pyrazine
- 54 123-32-0 → Dimethyl Pyrazine: 2,5-Dimethyl Pyrazine
- 55 625-84-3 → Dimethyl Pyrrole: 2,5-Dimethyl Pyrrole
- 56 3658-80-8 → Dimethyl Trisulfide
- 57 4747-07-3 → Diola
- 58 101-84-8 → Diphenyl Oxide
- 59 105-54-4 → Ethyl Butyrate
- 60 105-37-3 → Ethyl Propionate
- 61 13925-00-3 → 2-Ethyl Pyrazine (Lower Concentration)
- 62 13925-00-3 → 2-Ethyl Pyrazine (Higher Concentration)
- 63 470-82-6 → Eucalyptol
- 64 97-53-0 → Eugenol
- 65 67634-15-5 → Floralozone
- 66 6413-10-1 → Fructose
- 67 98-01-1 → Furfural
- 68 98-02-2 → Furfuryl Mercaptan
- 69 88683-93-6 → Grisalva
- 70 90-05-1 → Guaiacol
- 71 111-71-7 → Heptanal
- 72 111-70-6 → Heptanol: 1-Heptanol
- 73 68-25-1 → Hexanal
- 74 142-62-1 → Hexanoic acid
- 75 111-27-3 → Hexanol: 1-Hexanol
- 76 623-37-0 → Hexanol: 3-Hexanol
- 77 6728-26-3 → Hexenal: trans-1-Hexenal
- 78 111-26-2 → Hexyl Amine (Lower Concentration)
- 79 111-26-2 → Hexyl Amine (Higher Concentration)
- 80 101-86-0 → Hexyl Cinnamic Aldehyde
- 81 90-87-9 → Hydratropic Aldehyde Dimethyl Acetal
- 82 107-75-5 → Hydroxy Citronellal

| | | |
|-----|------------|--|
| 83 | 120-72-9 | → Indole |
| 84 | 67801-36-9 | → Indolene |
| 85 | 75-47-8 | → Iodoform |
| 86 | 14901-07-6 | → Ionone: beta-Ionone (Lower Concentration) |
| 87 | 14901-07-6 | → Ionone: beta-Ionone (Higher Concentration) |
| 88 | 79-69-6 | → Irone: alpha-Irone |
| 89 | 126-91-0 | → Linalool |
| 90 | 138-86-3 | → Limonene: d-Limonene |
| 91 | 31906-04-4 | → Lyrar |
| 92 | 67258-87-1 | → Maritima |
| 93 | 106-72-9 | → Melonal |
| 94 | 2216-51-5 | → Menthol: l-Menthol |
| 95 | 93-04-9 | → Methoxy-Naphthalene: 2-Methoxy Naphthalene |
| 96 | 134-20-3 | → Methyl Anthranilate |
| 97 | 462-95-3 | → Methyl Acetaldehyde Dimethyl Acetal |
| 98 | 1334-76-5 | → Methyl Furoate |
| 99 | 2271-428 | → Methyl-iso-Borneol: 2-Methyl-iso-Borneol |
| 100 | 491-35-0 | 0→ Methyl Quinoline: para-Methyl Quinoline |
| 101 | 2459-09-8 | 1→ Methyl iso-Nicotinate |
| 102 | 119-36-8 | 2→ Methyl Salicylate |
| 103 | 2432-51-1 | 3→ Methyl Thiobutyrate |
| 104 | 1222-05-5 | 4→ Musk Galaxolide |
| 105 | 1508-02-1 | 5→ Musk Tonalid |
| 106 | 37677-14-8 | 6→ Myracaldehyde |
| 107 | 143-13-5 | 7→ Nonyl Acetate |
| 108 | 4674-50-4 | 8→ Nootkatone |
| 109 | 111-87-5 | 9→ Octanol: 1-Octanol |
| 110 | 3391-86-4 | 0→ Octenol: 1-Octen-3-OL |
| 111 | 109-52-4 | 1→ Pentanoic Acid |
| 112 | 591-80-0 | 2→ Pentenoic Acid: 4-Pentenoic Acid |
| 113 | 103-82-2 | 3→ Phenyl Acetic Acid |
| 114 | 536-74-3 | 4→ Phenyl Acetylene |
| 115 | 60-12-8 | 5→ Phenyl Ethanol (Lower Concentration) |
| 116 | 60-12-8 | 6→ Phenyl Ethanol (Higher Concentration) |
| 117 | 78-59-1 | 7→ Phorone: iso-Phorone |
| 118 | 80-56-8 | 8→ Pinene: alpha-Pinene |
| 119 | 105-66-8 | 9→ Propyl Butyrate |
| 120 | 135-79-5 | 0→ Propyl Quinoline: iso-Propyl Quinoline |
| 121 | 111-47-7 | 1→ Propyl Sulfide |
| 122 | 110-86-1 | 2→ Pyridine |
| 123 | 94-59-7 | 3→ Safrole |
| 124 | 69460-08-8 | 4→ Sandiff |
| 125 | 115-71-9 | 5→ Santalol |
| 126 | 83-34-1 | 6→ Skatole |
| 127 | 10482-56-1 | 7→ Terpeneol, mostly alpha-Terpeneol |
| 128 | 110-01-0 | 8→ Tetrahydro Thiophene |

| | | |
|-----|------------|---------------------------------------|
| 129 | 91-61-2 | 9→ Tetraquinone |
| 130 | 36267-71-7 | 0→ Thienopyrimidine |
| 131 | 123-93-3 | 1→ Thioglycolic Acid |
| 132 | 110-02-1 | 2→ Thiophene |
| 133 | 89-83-8 | 3→ Thymol |
| 134 | 529-20-4 | 4→ Tolualdehyde: ortho-Tolualdehyde |
| 135 | 108-88-3 | 5→ Toluene (Lower Concentration) |
| 136 | 108-88-3 | 6→ Toluene (Higher Concentration) |
| 137 | 75-50-3 | 7→ Trimethyl Amine |
| 138 | 104-67-6 | 8→ Undecalactone: gamma-Undecalactone |
| 139 | 112-38-9 | 9→ Undecylenic Acid |
| 140 | 590-86-3 | 0→ Valeraldehyde: iso-Valeraldehyde |
| 141 | 503-74-2 | 1→ Valeric Acid: iso-Valeric Acid |
| 142 | 108-29-2 | 2→ Valerolactone: gamma-Valerolactone |
| 143 | 121-33-5 | 3→ Vanillin |
| 144 | 122-48-5 | 4→ Zingerone |

2. Perceptual descriptors

- 1 FRUITY, CITRUS
- 2 LEMON
- 3 GRAPEFRUIT
- 4 ORANGE
- 5 FRUITY, OTHER THAN CITRUS
- 6 PINEAPPLE
- 7 GRAPE JUICE
- 8 STRAWBERRY
- 9 APPLE (FRUIT)
- 10 PEAR
- 11 CANTALOUPE, HONEY DEW MELON
- 12 PEACH (FRUIT)
- 13 BANANA
- 14 FLORAL
- 15 ROSE
- 16 VIOLETS
- 17 LAVENDER
- 18 COLOGNE
- 19 MUSK
- 20 PERFUMERY
- 21 FRAGRANT
- 22 AROMATIC
- 23 HONEY
- 24 CHERRY (BERRY)
- 25 ALMOND
- 26 NAIL POLISH REMOVER
- 27 NUTTY (WALNUT ETC)
- 28 SPICY
- 29 CLOVE
- 30 CINNAMON
- 31 LAUREL LEAVES
- 32 TEA LEAVES
- 33 SEASONING (FOR MEAT)
- 34 BLACK PEPPER
- 35 GREEN PEPPER
- 36 DILL
- 37 CARAWAY
- 38 OAK WOOD, COGNAC
- 39 WOODY, RESINOUS
- 40 CEDARWOOD
- 41 MOTHBALLS
- 42 MINTY, PEPPERMINT
- 43 CAMPHOR
- 44 EUCALIPTUS

| | |
|----|--------------------------|
| 45 | CHOCOLATE |
| 46 | VANILLA |
| 47 | SWEET |
| 48 | MAPLE SYRUP |
| 49 | CARAMEL |
| 50 | MALTY |
| 51 | RAISINS |
| 52 | MOLASSES |
| 53 | COCONUT |
| 54 | ANISE (LICORICE) |
| 55 | ALCOHOLIC |
| 56 | ETHERISH, ANAESTHETIC |
| 57 | CLEANING FLUID |
| 58 | GASOLINE, SOLVENT |
| 59 | TURPENTINE (PINE OIL) |
| 60 | GERANIUM LEAVES |
| 61 | CELERY |
| 62 | FRESH GREEN VEGETABLES |
| 63 | CRUSHED WEEDS |
| 64 | CRUSHED GRASS |
| 65 | HERBAL, GREEN, CUT GRASS |
| 66 | RAW CUCUMBER |
| 67 | HAY |
| 68 | GRAINY (AS GRAIN) |
| 69 | YEASTY |
| 70 | BAKERY (FRESH BREAD) |
| 71 | SOUR MILK |
| 72 | FERMENTED (ROTTEN) FRUIT |
| 73 | BEERY |
| 74 | SOAPY |
| 75 | LEATHER |
| 76 | CARDBOARD |
| 77 | ROPE |
| 78 | WET PAPER |
| 79 | WET WOOL, WET DOG |
| 80 | DIRTY LINEN |
| 81 | STALE |
| 82 | MUSTY, EARTHY, MOLDY |
| 83 | RAW POTATO |
| 84 | MOUSE |
| 85 | MUSHROOM |
| 86 | PEANUT BUTTER |
| 87 | BEANY |
| 88 | EGGY (FRESH EGGS) |
| 89 | BARK, BIRCH BARK |
| 90 | CORK |

91 BURNT, SMOKY
92 FRESH TOBACCO SMOKE
93 INCENSE
94 COFFEE
95 STALE TOBACCO SMOKE
96 BURNT PAPER
97 BURNT MILK
98 BURNT RUBBER
99 TAR
100 CREOSOTE
101 DISINFECTANT, CARBOLIC
102 MEDICINAL
103 CHEMICAL
104 BITTER
105 SHARP, PUNGENT, ACID
106 SOUR, VINEGAR
107 SAUERKRAUT
108 AMMONIA
109 URINE
110 CAT URINE
111 FISHY
112 KIPPERY (SMOKED FISH)
113 SEMINAL, SPERM
114 NEW RUBBER
115 SOOTY
116 BURNT CANDLE
117 KEROSENE
118 OILY, FATTY
119 BUTTERY, FRESH BUTTER
120 PAINT
121 VARNISH
122 POPCORN
123 FRIED CHICKEN
124 MEATY (COOKED, GOOD)
125 SOUPY
126 COOKED VEGETABLES
127 RANCID
128 SWEATY
129 CHEESY
130 HOUSEHOLD GAS
131 SULFIDIC
132 GARLIC, ONION
133 METALLIC
134 BLOOD, RAW MEAT
135 ANIMAL
136 SEWER

- 137 PUTRID, FOUL, DECAYED
- 138 FECAL (LIKE MANURE)
- 139 CADAVEROUS (DEAD ANIMAL)
- 140 SICKENING
- 141 DRY, POWDERY
- 142 CHALKY
- 143 LIGHT
- 144 HEAVY
- 145 COOL, COOLING
- 146 WARM

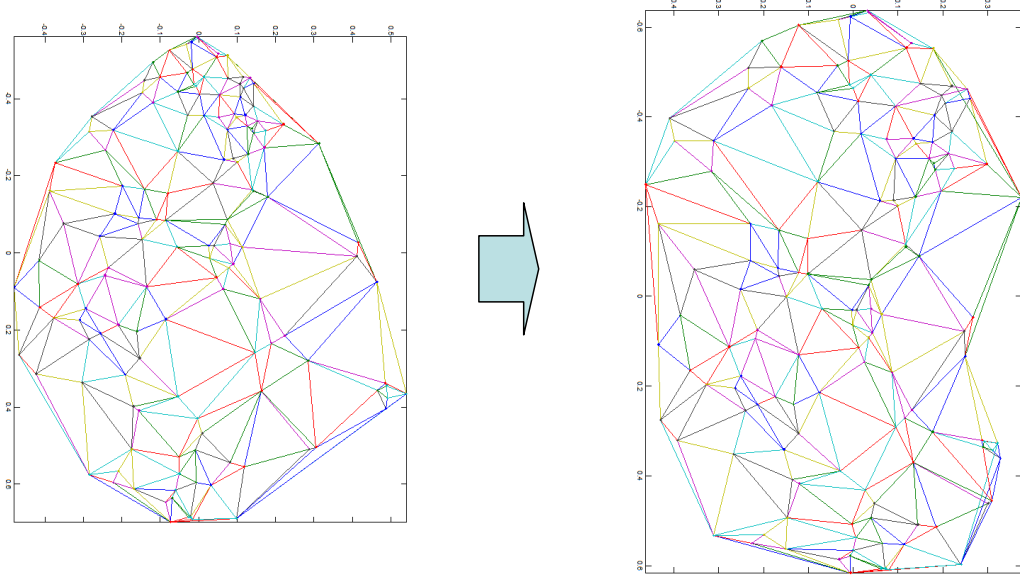
List of physico-Chemical parameters used

| | |
|----|------------------------------|
| 1 | C |
| 2 | H |
| 3 | O |
| 4 | N |
| 5 | S |
| 6 | I |
| 7 | L |
| 8 | molecular_weight |
| 9 | molecular_volume |
| 10 | molecular_length |
| 11 | molecular_width |
| 12 | molecular_depth |
| 13 | density |
| 14 | surface_area |
| 15 | Log_Kow_fragments |
| 16 | HLB |
| 17 | solubility_parameter |
| 18 | dispersion_3D |
| 19 | polarity_3D |
| 20 | hydrogen_bond_3D |
| 21 | hydrogen_bond_acceptor |
| 22 | hydrogen_bond_donor |
| 23 | dipole_moment_debye |
| 24 | hydrophilic_surface_area |
| 25 | water_of_hydration |
| 26 | boiling_point_C |
| 27 | vapor_pressure_torr |
| 28 | MR |
| 29 | parachor |
| 30 | connectivity_0 |
| 31 | connectivity_1 |
| 32 | connectivity_2 |
| 33 | connectivity_3 |
| 34 | connectivity_4 |
| 35 | valence_0 |
| 36 | valence_1 |
| 37 | valence_2 |
| 38 | valence_3 |
| 39 | valence_4 |
| 40 | kappa_2 |
| 41 | log_water_solubility |
| 42 | Log_P__atom_based |
| 43 | Z_chain_length |
| 44 | glass_transition_temperature |

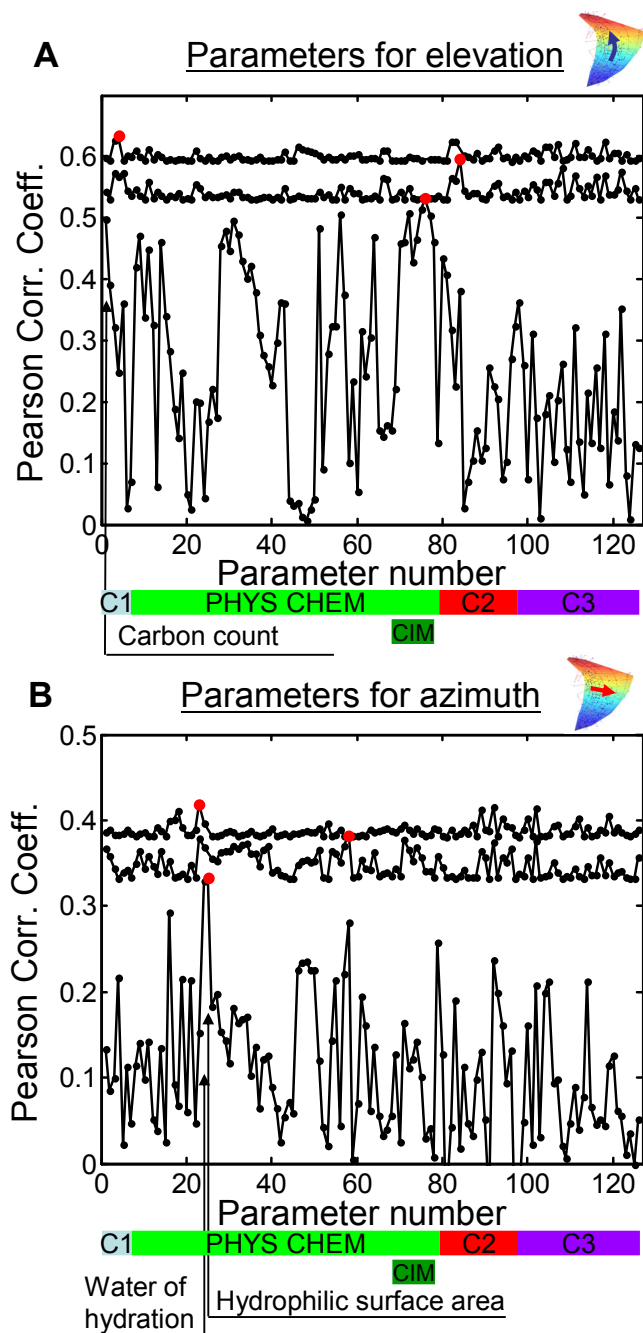
45 melt_transition_temperature
46 water_content_30_RH
47 water_content_50_RH
48 water_content_70_RH
49 water_content_90_RH
50 water_content_100_RH
51 molar_volume
52 Surface_tension
53 Viscosity_cp_at_25C
54 Surface_tension_in_water
55 Critical_Temperature_K
56 Critical_Pressure_bar
57 Normal_Boiling_Point_K
58 Normal_Freezing_Point_K
59 Enthalpy_of_formation
60 Gibbs_energy_of_formation
61 enthalpy_of_vaporization
62 enthalpy_of_fusion
63 liquid_viscosity
64 heat_capacity_25C
65 Effective_number_of_torsional_bonds
66 hydrogen_bond_number
67 Entropy_of_boiling_JKmol
68 Heat_capacity_change_on_boiling_JKmol
69 CIM_1
70 CIM_2
71 CIM_3
72 CIM_4
73 CIM_5
74 CIM_6
75 CIM_7
76 CIM_8
77 CIM_9
78 CIM_10
79 Polar_surface_area
80 C1C
81 C1H
82 C1O
83 C1N
84 C1S
85 C1I
86 C1L
87 H1O
88 H1N
89 H1S
90 S1S

| | |
|-----|-------|
| 91 | C2C |
| 92 | C2O |
| 93 | C2N |
| 94 | C3C |
| 95 | C3N |
| 96 | C1C1C |
| 97 | C2C1C |
| 98 | C1C1H |
| 99 | C2C1H |
| 100 | C3C1H |
| 101 | C1C1O |
| 102 | C1C2O |
| 103 | C2C1O |
| 104 | C1C1N |
| 105 | C1C2N |
| 106 | C1C3N |
| 107 | C2C1N |
| 108 | C1C1S |
| 109 | C2C1S |
| 110 | C2C1L |
| 111 | C1O1C |
| 112 | C1O1H |
| 113 | C1N1C |
| 114 | C2N1C |
| 115 | C1N1H |
| 116 | C1S1C |
| 117 | C1S1S |
| 118 | H1C1O |
| 119 | H1C2O |
| 120 | H1C1N |
| 121 | H1C2N |
| 122 | H1C1S |
| 123 | O1C1O |
| 124 | O2C1O |
| 125 | O1C1S |
| 126 | S1S1S |

The data above contains atom counts per molecule (C through L (chlorine)), number of pairs per molecule (C1C or C-C through C3N or C \equiv N), and numbers of triples per molecule (C1C1C for C-C-C through S-S-S).



Supplementary Figure 1. Equilibrating the density of the odorants in two dimensions. Left: the original set of odorants projected onto a flat 2D space and Delaunay triangulated. Right: the same set of odorants after relaxing the elastic energy of edges that are assumed to be springs with unit equilibrium length and the same elastic coefficient. The transformation (arrow) was constrained to be of the second order as in equation (1) of the main text. The final two coordinates were used to correlate with the structural and physico-chemical parameters (Table 1, Supplementary figure 2).



Supplementary Figure 2. The results of greedy algorithm for elevation (A) and azimuth (B) variables on the 2D fit to psychophysical data. Pearson correlation coefficient is shown as a function of the number of physico-chemical/structural parameter (see above). Three iterations are shown for each parameter by three lines with dots. The parameters yielding maximal correlation on each iteration are shown by the red dots. Some parameters are highlighted, such as Carbon count ($R=0.50$), hydrophilic surface area ($R=0.33$), and water of hydration ($R=0.33$). Horizontal axis also contains marking indicating the corresponding block of parameters included: element counts (C1), Molecular modeling Pro physico-chemical parameters (PHYS CHEM), pairs counts (C2), and triples counts (C3). CIM is the block of ten Burden chemical intuitive indexes.